Biophysical Chemistry 138 (2008) 138–143

Contents lists available at ScienceDirect

Biophysical Chemistry

journal homepage: http://www.elsevier.com/locate/biophyschem

Biophysical characterization of the interaction of p21 with calmodulin: A mechanistic study

Qiaoyun Shi, Xiaohui Wang, Jinsong Ren *

Division of Biological Inorganic Chemistry, State Key laboratory of Rare Earth Resources Utilization, Graduate School of the Chinese Academy of Sciences, Changchun Institute of Applied Chemistry, Chinese Academy of Sciences, Changchun, Jilin 130022, China

ARTICLE INFO

Article history:
Received 25 August 2008
Received in revised form 15 September 2008
Accepted 15 September 2008
Available online 20 September 2008

Keywords:
p21
Calmodulin
Dansyl
Tryptophan
Fluorescence quenching
Circular dichroism

ABSTRACT

p21 is a protein with important roles in cell proliferation, cell cycle regulation and apoptosis. Several studies have demonstrated that its intracellular localization plays an important role in the functional regulation and binding of calmodulin favors its nuclear translocation. However, the detail mechanism of the interaction with p21 and calmodulin is not well understood. In this report, peptides derived from the C-terminal of p21 that cover the binding domain of calmodulin were used to investigate the association of p21 with calmodulin. We found $p21^{141-164}$ interaction with Ca^{2+}-saturated dansyl-labelled calmodulin caused a significant increase in dansyl fluorescence intensity and a blue shift of the maximum emission from 510 to 475 nm. The Trp fluorescence intensities of mutated $p21^{141-164}$ peptides (F150W, Y151W and F159W) increased upon binding to Ca^{2+}-saturated calmodulin and fluorescence maxima were blue shifted from 350 nm to 330 nm. The results suggested $p21^{141-164}$ is most likely buried in the hydrophobic binding tunnel of calmodulin. Both dansyl and Trp fluorescence titrations generated dissociation constants around 0.1 μM and a stoichiometry of 1:1, which was further confirmed by nondenaturing gel band shift electrophoresis. Fluorescence titrations and Trp fluorescence quenching results indicated electrostatic interaction is involved in this association. Upon binding to calmodulin, $p21^{141-164}$ remained largely unstructured and showed only about 15% α-helix. In contrast to other calmodulin binding peptide, the dominant force in the association of $p21^{141-164}$ with calmodulin may be electrostatic interaction. Our results would be helpful for understanding the molecular details of p21 and calmodulin interaction.

1. Introduction

p21 is a protein with important roles in cell proliferation, cell cycle regulation, differentiation, senescence, and apoptosis [1–4]. It exhibits different functions in nuclear and cytoplasmic compartments [5]. Nuclear p21 induces a cycle arrest and inhibits DNA synthesis, functioning as a tumor suppressor [6,7], while cytoplasmic p21 has proliferation, anti-apoptosis and motility functions [8,9].

Calmodulin (CaM) is a Ca^{2+} binding protein and acts as transducer of the intracellular Ca^{2+} signal [10,11]. When bound to Ca^{2+}, CaM is able to bind to CaM-binding proteins and regulate their activity [12–14]. Agell et al. has demonstrated that Ca^{2+} saturated CaM can bind to the carboxyl-terminal domain of p21 [15] and that CaM binding favors the nuclear accumulation of p21 [16]. However, detail mechanism of this interaction is not clear, partly due to the lack of structural information. Herein, peptides derived from the C-terminal domain of p21 that cover the binding domain of the CaM were used to investigate the association of p21 with CaM. We found that $p21^{141-164}$ formed a 1:1 complex with Ca^{2+}-saturated CaM and the dissociation was around 0.1 μM. Surprisingly, $p21^{141-164}$ remained largely unstructured and showed only about 15% α-helix when bound to CaM. The results suggest the dominant force in the association of $p21^{141-164}$ with CaM may be electrostatic interaction. To the best of our knowledge, this is the first report that systematically characterizes the association of p21 with CaM.

2. Materials and methods

2.1. Peptide synthesis and protein preparation

Four peptides encompassing the putative CaM-binding domain of the C-terminal of p21 were chemically synthesized by the CL Bioscientific CO. LTD. The sequences were as follow: $p21^{141-164}$, KRRQTSMTDFYHSKRRLIFSKRKP; F150W, KRRQTSMTD*W*YHSKRRLIFSKRKP, substituting F150 of $p21^{141-164}$ with W; Y151W, KRRQTSMTDF*W*HSKRRLIFSKRKP, substituting Y151 of $p21^{141-164}$ with W; F159W, KRRQTSMTDFYHSKRRLI*W*SKRKP, substituting F159 of $p21^{141-164}$ with W. The purity of peptides was 95% according to high pressure liquid chromatography. The concentrations of all the

* Corresponding author. Tel.: +86 431 8526 2625; fax: +86 431 85262656.
E-mail address: jren@ciac.jl.cn (J. Ren).

0301-4622/$ – see front matter © 2008 Elsevier B.V. All rights reserved.
doi:10.1016/j.bpc.2008.09.012

peptides were determined by using a molar extinction coefficient (ε_{280}^{Trp}=5690 M^{-1} cm^{-1}, ε_{280}^{Tyr}=1280 M^{-1} cm^{-1}, ε_{280}^{Phe}=197 M^{-1} cm^{-1}). Recombinant mammalian CaM was expressed and purified as described previously [17], and the CaM concentration was determined by using the molar extinction coefficient of 3240 M^{-1} cm^{-1} at 276 nm.

2.2. Dansylation of CaM (Dans-CaM)

CaM was labeled with dansyl chloride according to the method described by Kincaid et al. [18]. Briefly, CaM was dissolved in 20 mM $NaHCO_3$, 100 mM NaCl, 250 μM $CaCl_2$, pH 10.0 to a final concentration of 1 mg/mL. To 2 mL of this material, 30 μL of 6 mM dansyl chloride (1.5 mol/mol of calmodulin) was added with stirring. After incubation in the dark for 2 h on ice, the mixture was dialyzed exhaustively against 250 mM NaCl, 5 mM $MgC1_2$, 100 μM EGTA, 20 mM Tris–HCl, pH 8.0, at 4 °C. Dans-CaM was stored as a lyophilized powder after exhaustive dialysis against distilled water.

2.3. Nondenaturing-polyacrylamide gel mobility shift

Nondenaturing-polyacrylamide gel mobility shift electrophoresis was performed following the procedure described previously [19]. Slab gels were composed of 15% acrylamide, 0.375 M Tris–HCl, pH 8.8, and 1 mM $CaCl_2$. After electrophoresis, the gels were stained by Coomassie Brilliant Blue G-250 staining solution (0.1% Coomassie Brilliant Blue G-250, 4% H_3PO_4, 10% $(NH_4)_2SO_4$, 20% ethanol). Images were photographed using a UVP gel documentation system (Ultra-violet Products, Upland, CA, USA).

2.4. Fluorescence measurements

Measurements of fluorescence were taken in a Jasco FP6500 spectrofluorometer using a 1 cm path length quartz cuvette. The cell holder was maintained at constant temperature by circulating water from a constant temperature water bath. The slits were set at 5 and 10 nm for excitation and emission. For intrinsic Trp fluorescence measurements, the excitation wavelength of 295 nm was used, while for dansyl fluorescence measurements, the excitation wavelength was 340 nm. Appropriate blank spectra were recorded on the buffer components and subtracted from spectra obtained on the samples. Fluorescence was also corrected by the relation, $F_{corr}=F_{obs}$ antilog $(OD_{ex}+OD_{em})/2$ for the inner filter effect when necessary, where OD_{ex} and OD_{em} are the optical densities at excitation and emission wavelengths, respectively.

The fluorescence titration data were fit to a single hyperbolic isotherm:

$$F = F_0 + \Delta F_{max}\left\{\frac{K_d + [B]_{total} + n[A]_{total}}{2n[A]_{total}}\right\} - \Delta F_{max}\sqrt{\left(\frac{K_d + [B]_{total} + n[A]_{total}}{2n[A]_{total}}\right)^2 - \frac{[B]_{total}}{2n[A]_{total}}}$$

arising from the equilibrium $A+B=AB$ which was generated by Mathtype 6.0. Where $[A]_{total}$ is the fixed concentration of the protein being titrated; $[B]_{total}$ is the final concentration of the ligand; F and F_0 are the fluorescence intensities of A in the presence and absence of B, respectively; $\Delta F_{max}=F_{max}-F_o$, F_{max} being the fluorescence intensity in the presence of the saturating concentrations of B; n is the A–B binding stoichiometry.

2.5. Fluorescence quenching experiments

In order to probe the microenvironment of bound $p21^{141-164}$, quenching of intrinsic Trp fluorescence by I^-, Cs^+, or acrylamide was examined. In experiments employing NaI and CsCl as a quencher, ionic strength was kept constant by the addition of NaCl. The data were analyzed using the Stern–Volmer Eq.: $F_0/F=1+K_{sv}[X]$, where F_0 and F are the fluorescence in the absence and presence of quencher, respectively; $[X]$ is the concentration of quencher; K_{sv} is the Stern–Volmer constant. The electrostatic parameter E, which is sensitive to the charge in the microenvironment around the fluorophore, was determined according to Eq.: $E=K_{sv-}/K_{sv+}$, where K_{sv-} and K_{sv+} are the Stern–Volmer constants for the negative (e.g. I^-) and positive (e.g. Cs^+) quenchers, respectively. In particular, values greater than 2.6 are typical for a positive charged environment [20]. Fluorescence quantum yields were determined by Eq.: $Q_x=Q_{st}(F_x/A_x)(A_{st}/F_{st})$, where Q_x, F_x and A_x are the emission quantum yield, the emission intensity at λ and the absorbance at the excitation wavelength, respectively, for the sample; Q_{st}, F_{st} and A_{st} are the parameters for the reference standard L-Trp [21]. The parameter L reflecting the fraction of chromophore accessible in protein compared with that of free L-Trp, is determined from Eq.: $L=(K_{sv}^{p}/K_{sv}^{Trp})\times(Q^{Trp}/Q^{p})$, where K_{sv}^{Trp} and K_{sv} are the Stern–Volmer constants for free L-Trp and protein Trp residues, respectively; Q^{Trp} and Q are the emission quantum yield for free L-Trp and protein Trp residues, respectively [22]. L-Trp was chosen as a reference standard. K_{sv}^{Trp} values of 9.10 M^{-1} for I^- [22], 2.80 M^{-1} for Cs^+ [22] and 14.5 M^{-1} for acrylamide [23] and a Q^{Trp} value of 0.200 [23] were used for calculations.

2.6. Circular Dichroism spectra measurements

Circular Dichroism (CD) spectra were recorded on a Jasco-810 spectropolarimeter at 25 °C. The optical chamber of CD spectrometer was deoxygenated with dry purified nitrogen (99.99%) for 45 min before use and kept the nitrogen atmosphere during experiments. Four scans were accumulated and automatically averaged. Scan speed was set to 20 nm/min with 4 s response time, 0.1 nm data pitch and 1 nm bandwidth. Far UV CD spectra (195–260 nm) were acquired using a cell path length of 0.1 cm and the results were expressed as mean residue ellipticity $[\theta]_\lambda$ in deg cm^2 $dmol^{-1}$ at a given wavelength λ (nm) using the relation: $[\theta]_\lambda=\theta_\lambda M_o/10\ c\ l$, where θ_λ is the observed ellipticity in millidegrees at wavelength λ, M_o is the mean residue weight of the protein, c is the protein concentration (mg/cm^3), and l is the path length (cm). It should be noted that each observed θ_λ of the protein was corrected for the contribution of the buffer. The α-helical content was calculated using Eq.: α-Helix (%)=$-([\theta]_{222\ nm}+2340)/30{,}300\times100$ [24].

3. Results

3.1. Dans-CaM fluorescence analysis

The dansyl chromophore covalently bound to CaM is a very sensitive probe to study the interaction between CaM and its binding proteins [25,26]. As shown in Fig. 1, the addition of $p21^{141-164}$ to the Ca^{2+} saturated Dans-CaM (Dans-CaM/Ca^{2+}) caused a significant increase in the danysl fluorescence intensity and a blue shift of the maximum emission spectrum from 510 to 475 nm, indicating that dansyl entered a more hydrophobic environment [25,26]. Titration of Dans-CaM/Ca^{2+} with $p21^{141-164}$ gave a hyperbolic plot and a value of 1.0 was obtained for n by fitting the data, which was further confirmed by nondenaturing gel band shift electrophoresis that directly demonstrated $p21^{141-164}$ formed 1:1 complex with Ca^{2+} saturated CaM (CaM/Ca^{2+}) (Fig. 2A). However, no fluorescence change of apo-Dans-CaM was observed upon the addition of $p21^{141-164}$, supporting the notion that the association of $p21^{141-164}$ with CaM is Ca^{2+} dependent (Fig. S1). As shown in Table 1, no significant differences in affinities of $p21^{141-164}$–Dans-CaM/Ca^{2+} were observed during the pH range of 5.8–8.5, whereas ionic strength markedly affected the association of $p21^{141-164}$ with Dans-CaM/Ca^{2+}. At concentrations of 0.1–0.4 M NaCl, the values of K_d were significantly increased from 0.15 μM to 10.2 μM, suggesting that electrostatic interactions contribute to the $p21^{141-16}$–CaM interaction.

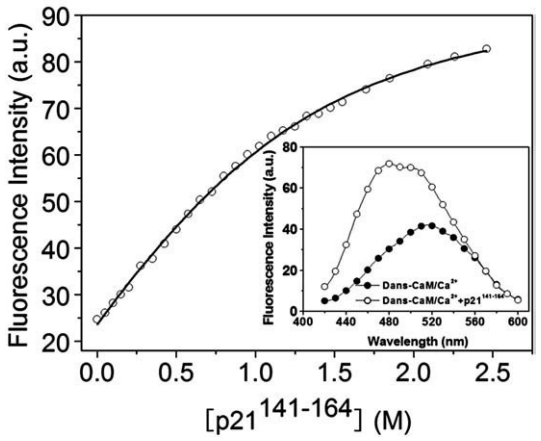

Fig. 1. Titration curve of Dans-CaM/Ca^{2+} with $p21^{141-164}$. Dans-CaM was 0.75 μM in 20 mM Tris, 100 mM NaCl, and 1 mM $CaCl_2$, pH 7.4. The excitation wavelength was 340 nm and Dansyl fluorescence was monitored at fixed wavelength of 480 nm. Curve was fitted according to the method described in Materials and methods. A K_d of 0.15 ± 0.08 μM and an n of 1.15 ± 0.12 were obtained. Insets were fluorescence spectra of Dans-CaM/Ca^{2+} and $p21^{141-164}$–Dans-CaM/Ca^{2+} complex.

3.2. Mutated $p21^{141-164}$ Trp fluorescence measurements

Trp fluorescence is one of the most widely used tools to probe and determine the conformational change of proteins during binding of various ligands [27]. Since $p21^{141-164}$ has no natural Trp residues, F150W, Y151W and F159W were synthesized. This approach is facilitated by the absence of Trp residues in CaM. As shown in Fig. S2, the far UV CD spectra of the three mutants almost resemble that of $p21^{141-164}$, showing that the single amino acid substitution did not marginally affect the secondary structure. Nondenaturing gel band shift electrophoresis indicated that F150W, Y151W and F159W formed 1:1 complex with CaM (Fig. 2B). Moreover, titrations of Dans-CaM with three mutated peptides suggested that the single mutation did not compromise their CaM-binding ability compared to that of $p21^{141-164}$ (K_d 0.10 μM for F150W–Dans-CaM; 0.14 μM for Y151W–Dans-CaM; 0.15 μM for F159W-Dans-CaM. Fig. S3). Hence, mutated $p21^{141-164}$ peptides Trp intrinsic fluorescence could be used as a probe to investigate the association of $p21^{141-164}$ with CaM.

As shown in Fig. 3, after excitation at 295 nm, where the Trp side chains are selectively excited, the fluorescence spectrum of F150W had maxima at 350 nm, which is typical for solvent-exposed Trp side chains in polar environment [28]. When F150W associated with CaM/Ca^{2+}, its fluorescence intensity increased and fluorescence maximum was considerably blue shifted to 330 nm in the complexes, indicating the Trp residue moving to a hydrophobic environment. As suggested by many other CaM-binding peptides, such as MLCK peptide [29,30], Trp residue of F150W was most likely buried in the hydrophobic binding pocket of CaM. It should be noted here that no Trp fluorescence change of three mutant peptides was observed upon the addition of apo-CaM (Fig. S4).

Analysis of the titration curve of F150W with CaM/Ca^{2+} showed that F150W associated with CaM/$Ca^{2+}$with a K_d of 0.12 ± 0.03 μM and 1:1 stoichiometry, further supporting the results obtained by dansyl fluorescence and nondenaturing-polyacrylamide gel mobility shift electrophoresis. Similar results were observed for Y151W and F159W (Fig. S5. Y151W: K_d = 0.09 ± 0.03 μM and n = 1.13 ± 0.10, F159W: K_d = 0.13 ± 0.02 μM and n = 1.06 ± 0.07). The dissociation constants for F150W and CaM/Ca^{2+} in varying conditions were shown in Table 2, which were in good agreement with those obtained by dansyl fluorescence. To further confirm the speculation that $p21^{141-164}$ associated with CaM by binding to its hydrophobic pocket, calmidazolium, an anti-CaM drug which binds tightly to Ca^{2+}-induce hydrophobic site of CaM [31], was used to compete with F150W for the association with CaM. The data showed that

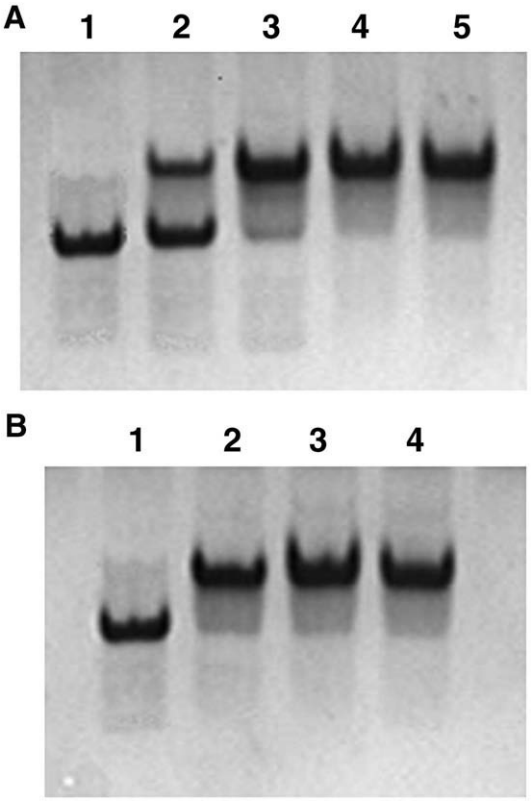

Fig. 2. Nondenaturing-polyacrylamide gel mobility shift characterization of the interaction p21 with CaM/Ca^{2+}. (A), Lane 1, CaM/Ca^{2+}; lane 2, 0.5:1 F150W–CaM/Ca^{2+}; lane 3, 1:1 F150W–CaM/Ca^{2+}; lane 4, 1.5:1 F150W–CaM/Ca^{2+}; lane 5, 2:1 F150W–CaM/Ca^{2+}. (B) Lane 1, CaM/Ca^{2+}; lane 2, 1:1 F150W–CaM/Ca^{2+}; lane 3, 1:1 Y151W–CaM/Ca^{2+}; lane 4, 1:1 F159W–CaM/Ca^{2+}.

calmidazolium significantly inhibited the affinity of F150W for CaM/Ca^{2+} in a dose dependent manner. The results suggested that $p21^{141-164}$ binds to the hydrophobic tunnel of CaM and hydrophobic interaction contributes to this association.

In order to determine the effect of pH and temperature on the stability of $p21^{141-164}$–CaM complex, wavelengths of maximum emission (λ_{max}) of Trp were monitored at varying pH and temperature. As shown in Fig. 4A, F150W–CaM complex were stable during the pH range of 5.5–9.5, which was consistent with previous dansyl fluorescence titration results. At more acidic or basic pH values, λ_{max} was gradually shifted from 330 nm to 350 nm, indicative of the dissociation of complex. Fig. 4B revealed that F150W–CaM complex were stable below 35 °C, while the affinity of the complex was dramatically weakened when the temperature was greater than 40 °C.

3.3. Fluorescence quenching analysis

Fluorescent quenching has been widely used for studying the degree of exposure and environment of aromatic amino acid residues.

Table 1
Dissociation constants for the interaction of $p21^{141-164}$ with Dans-CaM/Ca^{2+} under varying conditions at 25 °C determined by dansyl fluorescence titrations

NaCl (M)	pH	K_d (μM)
0.1	7.4	0.15 ± 0.08
0.2	7.4	0.47 ± 0.02
0.3	7.4	1.87 ± 0.21
0.4	7.4	10.15 ± 0.11
0.1	8.5	0.17 ± 0.01
0.1	5.8	0.37 ± 0.19

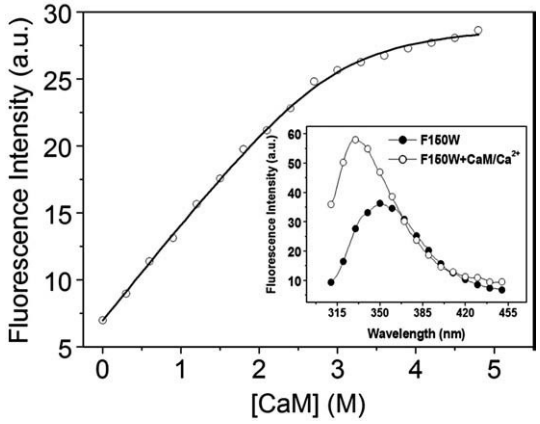

Fig. 3. Titration curve of F150W with CaM/Ca^{2+}. F150W was 1.0 μM in 20 mM Tris, 100 mM NaCl, and 1 mM $CaCl_2$, pH 7.4. The excitation wavelength was 295 nm and Trp fluorescence was monitored at fixed wavelength of 350 nm. Curve was fitted according to the method described in Materials and methods. A K_d of 0.12 ± 0.03 μM and an n of 1.10 ± 0.12 were obtained. Insets were Trp fluorescence spectra of F150W and F150W–CaM/Ca^{2+} complex.

Acrylamide is an efficient neutral quencher of Trp fluorescence and can penetrate the protein matrix. In contrast, the ionic quenchers are hydrated and cannot diffuse into the protein molecule. To probe the detailed microenvironment of binding interface between p21 and CaM, we examined iodide, Cs^+ and acrylamide quenching of Trp fluorescence of mutated $p21^{141-164}$ peptides and CaM/Ca^{2+} complex. As shown in Fig. 5, Trp fluorescence in F150W was more efficiently quenched than that of F150W–CaM/Ca^{2+}, irrespective of the nature of the quencher. Similar quenching properties were observed for Y151W and F159W (Fig. S6). The results indicated that the Trp residue most likely moved to the hydrophobic tunnel of CaM, which was in good agreement our previous result.

Fluorescence quenching parameters were summarized in Table 3. K_{sv} values of Trp in the mutated peptides were close to that of L-Trp, indicative of the completely exposed Trp residue. Moreover, E and L values showed that the Trp residues of each free mutated peptides were in a positively charged environment, which was consistent with the fact that many Lys and Arg residues are located around Trp residues in these mutated peptides. Upon binding to CaM/Ca^{2+}, K_{sv}, E and L decreased dramatically and no apparent differences of L values between charged and neutral quenchers were observed. The results indicated that CaM binding led to the shifting of microenvironment around the Trp residue from a positive charged one to a neutral one and suggested that electrostatic interactions are involved in the $p21^{141-164}$–CaM interaction, further substantiating previous fluorescence titration results.

Table 2
Dissociation constants for the interaction of F150W with CaM/Ca^{2+} under varying conditions at 25 °C determined by Trp fluorescence titrations

NaCl (M)	pH	Calmi− (μM)	K_d (μM)
0.1	7.4	0	0.12 ± 0.03
0.3	7.4	0	2.32 ± 0.07
0.4	7.4	0	10.41 ± 0.09
0.1	5.5	0	0.20 ± 0.10
0.1	9.5	0	0.47 ± 0.04
0.1	7.4	5.0	2.02 ± 0.14
0.1	7.4	10.0	3.52 ± 0.10

Calmi−: the anti-CaM drug Calmidazolium.

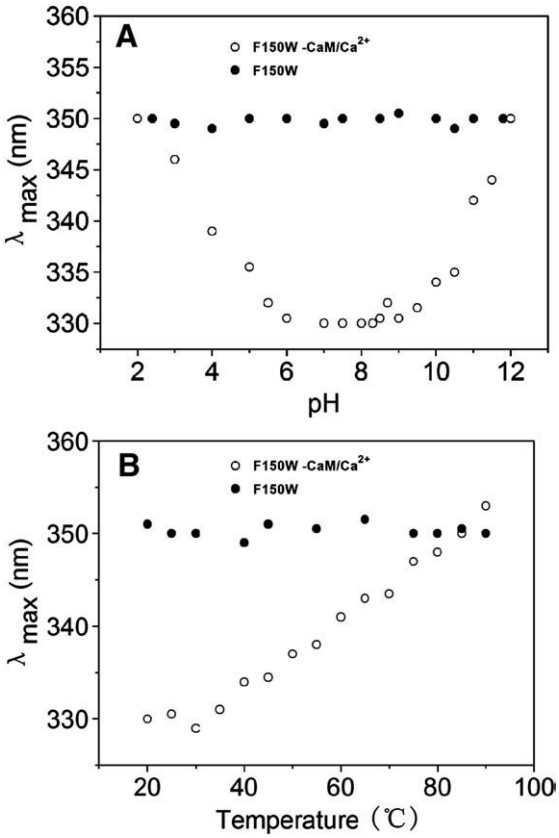

Fig. 4. Effect of pH (A) and temperature (B) on the stability of F150W–CaM/Ca^{2+} complex. F150W and CaM were 1.0 μM in 20 mM Tris, 100 mM NaCl, and 1 mM $CaCl_2$, pH 7.4. Wavelengths of maximum emission (λ_{max}) of Trp were monitored at varying pH and temperature.

3.4. Far UV CD measurements

It is recognized that CaM-binding peptide is induced into an amphipathic helix when binding to Ca^{2+} saturated CaM [29,30,32,33]. The conformational change of $p21^{141-164}$ induced by CaM was analyzed by far UV CD measurements, basing on the earlier conclusions that CaM/Ca^{2+} does not gain α-helical structure upon binding to its target peptides [29,30]. As shown in Fig. 6, the CD spectra of $p21^{141-164}$ showed an unordered structure, while CaM/Ca^{2+} exhibited spectra characteristic of α-helical conformation. The mean residue ellipticity of $p21^{141-164}$–CaM complex was greater than the weighted sum of those of $p21^{141-164}$ and CaM, indicating that $p21^{141-164}$ might be induced to adopt α-helical structure. The derived CD spectrum of bound $p21^{141-164}$ exhibited pronounced negative bands around 222nm and 208 nm and a positive band around 195 nm. Analysis of the data showed that CaM-binding $p21^{141-164}$ had 15% α-helix, which was much lower than that of most other CaM-binding peptides (40–50%) when bound to CaM/Ca^{2+} [29,30,32,33].

4. Discussion

p21 is a natively unfolded protein [34,35]. The conformational plasticity of C-terminal domain confers to p21 the ability to bind to multiple proteins by using essentially the same set of surface residues [36]. As suggested, this versatility appears to stem from the flexible use of a sequence that does not have any clear secondary structure propensity in solution and will adopt a secondary structure determined by the characteristics of the target proteins [36]. It has been reported that the C-terminal domain of p21 adopts an extended β-sheet structure when bound to PCNA [37].

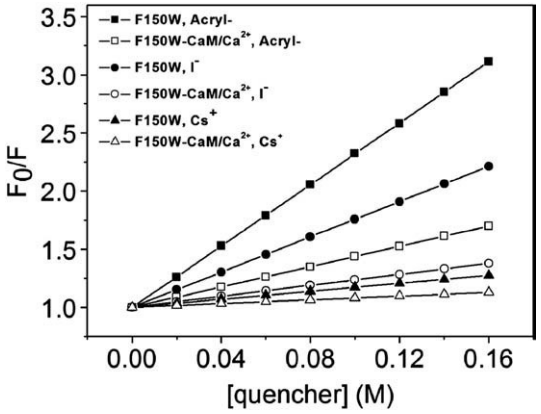

Fig. 5. Stern–Volmer plots for fluorescence quenching of Trp in F150W and F150W–CaM/Ca^{2+} complex with acrylamide, I^- and Cs^+ performed at 25 °C after excitation of the samples at 295 nm.

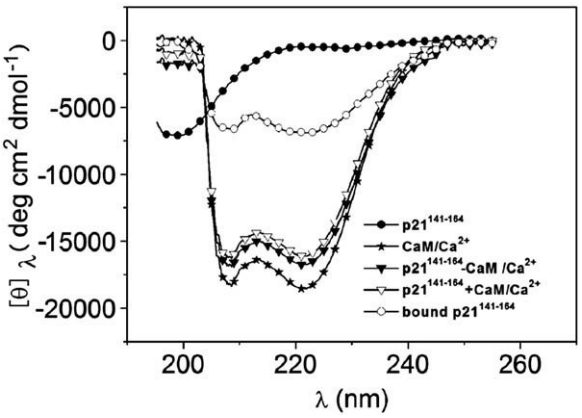

Fig. 6. Far UV CD spectra of CaM/Ca^{2+}, $p21^{141-164}$–CaM/Ca^{2+} complex and CaM-bound $p21^{141-164}$. $p21^{141-164}$ and CaM/Ca^2 were 50 μM in 20 mM Tris, 100 mM NaCl, and 1 mM $CaCl_2$, pH 7.4.

CaM is a ubiquitous protein that can regulate a number of different eukaryotic enzymes in a variety of cellular locations [12–14]. It is a dumb bell shaped protein molecule with two Ca^{2+} binding lobes. Each lobe of CaM contains two EF-hand (alpha helix-loop–alpha helix) motifs connected by a small antiparallel β-sheet between the two loops. Calcium binding results in the exposure of two hydrophobic pockets for target protein binding, surrounded by negatively charged residues [38–40]. Moreover, when CaM binds to CaM-binding proteins, the binding domain of these proteins is induced to fold into an amphipathic helix [29,30,32,33].

We note that $p21^{141-164}$ interaction with Dans-CaM/Ca^{2+} causes a significant increase in dansyl fluorescence intensity and a blue shift of the maximum emission from 510 to 475 nm. When mutated $p21^{141-164}$ peptides bind to CaM/Ca^{2+}, a characteristic blue shift and increase in fluorescence intensity is observed. Moreover, calmidazolium significantly inhibits the affinity of F150W for CaM/Ca^{2+} in a dose dependent manner. The results suggest that $p21^{141-164}$ most likely fit into the CaM-binding tunnel formed by two lobes in a similar way to many other CaM-binding peptides [29,30,40] and hydrophobic contacts within the core of the binding site tunnel contribute to this association. Meador et al. have identified the critical hydrophobic interaction as being due to the presence of at least two bulky hydrophobic residues in the CaM-binding segment separated by an 8 or 12 positions [30,40]. As for $p21^{141-164}$, the hydrophobic side chains of Phe-150 and Phe-159 may be involved in extensive hydrophobic contacts with the C- and N-terminal domains of CaM.

Table 3
Fluorescence quenching parameters for Trp residue in mutated $p21^{141-164}$ and mutated $p21^{141-164}$–CaM/Ca^{2+} complexes

Species	λ_{max} (nm)	Q	K_{sv} (M^{-1}) Acryl−	K_{sv} (M^{-1}) I^-	K_{sv} (M^{-1}) Cs^+	E	L	L	L
F150W	350	0.100	13.2	7.58	1.72	4.41	1.83	1.67	1.23
F150W–CaM	330	0.102	4.37	2.37	0.80	2.96	0.59	0.51	0.56
Y151W	351	0.106	12.6	6.89	1.20	5.74	1.64	1.43	0.8
Y151W–CaM	329	0.112	4.79	2.90	0.91	3.19	0.59	0.57	0.58
F159W	351	0.108	13.9	8.19	1.53	5.35	1.78	1.67	1.01
F159W–CaM	335	0.114	3.72	2.59	0.81	3.20	0.45	0.50	0.51
L-Trp	350	0.200[a]	14.5[a]	9.10[b]	2.80[b]	3.25	–	–	–

Acryl−: Acrylamide. λ_{max}, Q, K_{sv}, E, and L values refer to the wavelength of maximum fluorescence emission, quantumn yield, the Stern–Volmer constant, the electrostatic parameter (K_{sv-}/K_{sv+}), the fraction of chromophore access in protein respectively. L-Trp is chosen as a reference standard.
[a]Values obtained from Ref. [23].
[b]Values obtained from Ref. [22].

Fluorescence titrations have revealed that high salt markedly suppress the binding of $p21^{141-164}$ to CaM. The results indicate that electrostatic interaction is significantly involved in this association, which is further supported by Trp fluorescence quenching results that CaM binding leads to the shifting of microenvironment around Trp of the mutated $p21^{141-164}$ peptides from a positive charged one to a neutral one. Esteve et al. have shown that p21 $^{145-164}$ binds to CaM with apparent dissociation constant of 1.7 μM [36], more than an order of magnitude of that of p21 $^{141-164}$. Compared to $p21^{141-164}$, $p21^{145-164}$ lacks a positively charged region (KRRQ) and shows significant decrease in binding affinity for CaM, highlighting the importance of electrostatic features of CaM-$p21^{141-164}$ binding, especially the cluster of three basic residues at N-terminal.

Several studies have demonstrated that the binding surface of CaM and CaM-binding peptide corresponds to negatively charged margins separating a hydrophobic core [29,30,40]. The positively charged patch at the N-terminal of $p21^{141-164}$ peptide (position 1, 2 and 3) interacts strongly with the negatively charged Glu residues of CaM, favoring optimal orientation. Afshar et al. have suggested that negatively charged margins at the binding surface extremities interact strongly with positively charged residues separated by nine or ten positions [41]. His152 and Arg162 or Lys 163 of $p21^{141-164}$ may interact with residues from located in tunnel entrance margin of CaM and make a major contribution to the electrostatic energy.

The great flexibility of CaM when binding its target peptides has been readily demonstrated by many studies [10,42]. As suggested, $p21^{141-164}$ most likely binds CaM-binding tunnel in a similar way to many other CaM-binding peptides. However, in contrast to other CaM-binding peptides, which usually adopt a high content of α-helix (40–50%) when bound to Ca^{2+}-saturated calmodulin, p21 $^{141-164}$ remained largely unstructured and showed only about 15% α-helix when bound to calmodulin. The results indicate that the dominant feature of $p21^{141-164}$ and CaM-binding surface may not be the hydrophobic interaction which usually governs the binding of CaM and CaM-binding peptide. The dominant force in the association of $p21^{141-164}$ with CaM may be electrostatic interaction, which determines the orientation and strong binding of the peptide. This is consistent with the fact that $p21^{141-164}$ is a highly positively charged peptides (9 net positive charge/24 residues).

In conclusion, we systematically characterize the association of p21 with CaM in this study. $p21^{141-164}$ interaction with Dans-CaM/Ca^{2+} caused a significant increase in dansyl fluorescence intensity and a blue shift of the maximum emission from 510 to 475 nm. The Trp fluorescence intensities of mutated $p21^{141-164}$ peptides increased upon binding to CaM/Ca^{2+} and fluorescence maxima were blue shifted from 350 nm to 330 nm. These suggested $p21^{141-164}$ most likely binds

to the hydrophobic tunnel of CaM and hydrophobic interaction contributes to this association. Both dansyl and Trp fluorescence titrations generated dissociation constants around 0.1 μM and a stoichiometry of 1:1, which was further confirmed by nondenaturing gel band shift electrophoresis. Fluorescence titrations and Trp fluorescence quenching results indicated electrostatic interaction is involved in this association. Upon binding to CaM, p21 $^{141-164}$ remained largely unstructured and showed only about 15% α-helix. We speculate that the dominant force in the association of p21$^{141-164}$ with CaM may be electrostatic interaction. Our results would be helpful for understanding the molecular details of p21 and CaM interaction.

Acknowledgements

This project was supported by grants from the National Natural Science Foundation of China, the Fund from CAS and Jilin Province.

Appendix A. Supplementary data

Supplementary data associated with this article can be found, in the online version, at doi:10.1016/j.bpc.2008.09.012.

References

[1] W.S. El-Deiry, T. Tokino, V.E. Velculescu, D.B. Levy, R. Parsons, J.M. Trent, D. Lin, W.E. Mercer, K.W. Kinzler, B. Vogelstein, WAF1, a potential mediator of p53 tumor suppression, Cell 75 (1993) 817–825.
[2] A.L. Gartel, A.L. Tyner, The role of the cyclin-dependent kinase inhibitor p21 in apoptosis, Mol. Cancer Ther. 1 (2002) 639–649.
[3] A. Noda, Y. Ning, S.F. Venable, O.M. Pereira-Smith, J.R. Smith, Cloning of senescent cell-derived inhibitors of DNA synthesis using an expression screen, Exp. Cell Res. 211 (1994) 90–98.
[4] C.J. Sherr, J.M. Roberts, CDK inhibitors: positive and negative regulators of G1-phase progression, Genes Dev. 13 (1999) 1501–1512.
[5] O. Coquerer, New roles for p21 and p27 cell-cycle inhibitors: a function for each cell compartment? Trends Cell Biol. 13 (2003) 65–70.
[6] A. Rodriguez-Vilarrupla, C. Diaz, N. Canela, H.P. Rahn, O. Bachs, N. Agell, Identification of the nuclear localization signal of p21(cip1) and consequences of its mutation on cell proliferation, FEBS Lett. 531 (2002) 319–323.
[7] N.D. Perkins, Not just a CDK inhibitor: regulation of transcription by p21(Waf1/Cip1/Sdi1), Cell Cycle 1 (2002) 39–41.
[8] M. Asada, T. Yamada, H. Ichijo, D. Delia, K. Miyazono, K. Fukumuro, S. Muzutani, Apoptosis inhibitory activity of cytoplasmic p21(Cip1/Waf1) in monocytic differentiation, EMBO J. 18 (1999) 1223–1234.
[9] H. Tanaka, T. Yamada, M. Asada, S. Mizutani, H. Yoshikawa, M. Tohyma, Cytoplasmic p21Cip1/Waf1 regulates neurite remodling by inhibiting Rho-kinase activity, J. Cell Biol. 158 (2002) 321–329.
[10] D. Chin, A.R. Means, Calmodulin: a prototypical calcium sensor, Trends Cell Biol. 10 (2000) 322–328.
[11] A.R. Means, J.R. Dedman, Calmodulin—an intracellular calcium receptor, Nature 285 (1980) 73–77.
[12] M. Ikura, Calcium binding and conformational response in EF-hand proteins, Trends Biochem. Sci. 21 (1996) 14–17.
[13] C.B. Klee, T. Vanaman, Calmodulin, Adv. Protein Chem. 35 (1982) 213–321.
[14] H. Weinstein, E.L. Mehler, Ca^{2+} binding and structural dynamics in the functions of calmodulin, Annu. Rev. Physiol. 56 (1994) 213–236.
[15] M. Taules, A. Rodriguez-Vilarrupla, E. Rius, J.M. Estanyol, O. Casanovas, D.B. Sacks, E. Perez-Paya, O. Bachs, N. Agell, Calmodulin binds to p21(Cip1) and is involved in the regulation of its nuclear localization, J. Biol. Chem. 27 (274(35)) (1999) 24445–24448.
[16] A. Rodriguez-Vilarrupla, M. Jaumot, N. Abella, N. Canela, S. Brun, C. Diaz, J.M. Estanyol, O. Bachs, N. Agell, Binding of calmodulin to the carboxy-terminal region of p21 induces nuclear accumulation via inhibition of protein kinase C-mediated phosphorylation of Ser153, Mol. Cell. Biol. 25 (16) (2005) 7364–7374.
[17] M. Zhang, T. Yuan, J.M. Aramini, H.J. Vogel, An NMR study of the interaction between calmodulin and its binding domain of rat cerebellum nitric oxide synthase, J. Biol. Chem. 270 (1995) 20901–20907.
[18] R.L. Kincaid, M. Vaughan, J. Osborne, V.A. Tkachuk, Ca^{2+}-dependent interaction of 5-dimethylaminonaphthalene-1-sulfonyl-calmodulin with cyclic nucleotide phospho diesterase,calcineurin,and troponin I, J. Biol. Chem. 257 (1982) 10638–10643.
[19] V.G. Aldrin, A.B. Junor, J.V. Hans, Spectroscopic characterization of the interaction between calmodulin-dependent protein kinase I and calmodulin, Arch. Biochem. Biophys. 379 (2000) 28–36.
[20] F. Ricchelli, An investigation of the electronic environment of tryptophan in proteins: reliability of fluorescence quenching experiments, J. Photochem. Photobiol. B 7 (1990) 93–95.
[21] E.P. Kirby, R.F. Steiner, The tryptophan microenvironment in apomyoglobin, J. Biol. Chem. 245 (1970) 6300–6303.
[22] E.A. Burstein, Intrinsic protein fluorescence: origin and applications, Itogi Nauki Tekhn. Ser. Biofiz. 7 (1977) 138–161.
[23] F.W.J. Teale, G. Weber, Ultraviolet fluorescence of the aromatic amino acids, Biochem. J. 65 (1957) 476–482.
[24] Y.H. Chen, J.T. Yang, A new approach to the calculation of secondary structures of globular proteins by optical rotatory dispersion and circular dichroism, Biochem. Biophys. Res. Commun. 44 (1971) 1285–1291.
[25] T. Vorherr, P. James, J. Krebs, Interaction of calmodulin with the calmodulin binding domain of the plasma membrane Ca^{2+} pump, Biochemistry 29 (1990) 355–365.
[26] R.L. Kincaid, M.L. Billingsley, M. Vaughan, Preparation of fluorescent, cross-linking, and biotinylated calmodulin derivatives and their use in studies of calmodulin-actived phosphodiesterase and protein phosphatase, Methods Enzymol. 159 (1988) 625–626.
[27] J.R. Lakowicz, Principles of Fluorescence Spectroscopy, 2nd ed.Plenum Publishers, New York, 1999 10013.
[28] T.E. Creighton, Proteins: Structures and Molecular Properties, Second Ed.Freeman and Company, New York, 1993.
[29] M. Ikura, G.M. Clore, A.M. Gronenborn, G. Zhu, C.B. Klee, A. Bax, Solution structure of a calmodulin-target peptide complex by multidimensional NMR, Science 256 (1992) 632–638.
[30] W.E. Meador, A.R. Means, F.A. Quiocho, Target enzyme recognition by calmodulin: 2.4 Å structure of calmodulin–peptide complex, Science 257 (1992) 1251–1255.
[31] K. Geitzen, A. wuthrich, H. Bader, R 24571: a new powerful inhibitor of red blood cell Ca2+-transport ATPase and of calmodulin-regulated functions, Biochem. Biophys. Res. Commun. 101 (1981) 418–425.
[32] M. Ikura, A. Bax, Isotope filtered 2D NMR of protein–peptide complex: study of a skeletal muscle myosin light-chain kinase fragment bound to calmodulin, J. Am. Chem. Soc. 114 (1992) 2433–2440.
[33] S.M. Roth, D.M. Schneider, L.A. Strobel, M.F.A. Van Berkum, A.R. Means, A.J. Wand, Characterization of the secondary structure of calmodulin in complex with a calmodulin-binding domain peptide, Biochemistry 31 (1992) 1443–1451.
[34] R.W. Kriwacki, L. Hengst, L. Tennant, Structure studies of p21Waf1/Cip1/Sdi1 in the free and cdk2-bound state: conformation disorder mediated binding diversity, Proc. Natl. Acad. Sci. U. S. A. 93 (1996) 11504–11509.
[35] A.K. Dunker, J.D. Lawson, C.J. Brown, Intrinsically disordered protein, J. Mol. Graph. Model. 19 (2001) 26–59.
[36] V. Esteve, N. Canela, A. Rodriguez-Vilarrupla, R. Aligue, N. Agell, I. Mingarro, O. Bachs, E. Perez-Paya, The structural plasticity of the C terminus of p21Cip1 is a determinant for target protein recognition, Chem. Bio. Chem. 4 (2003) 863–869.
[37] J. Gulbis, Z. Kelman, E. Gibbs, J. Hurwitz, M. O'Donnell, J. Kuriyan, Structure of the C-terminal region of p21WAF1/CIP1 complexed with human PCNA, Cell 87 (1996) 297–306.
[38] H. Kuboniwa, N. Tjandra, S. Grzesiek, H. Ren, C.B. Klee, A. Bax, Solution structure of calcium-free calmodulin, Nat. Struct. Biol. 2 (1995) 768–776.
[39] M. Zhang, T. Tanaka, M. Ikura, Solution structure of apocalmodulin: conformational transition induced by calcium binding, Nat. Struct. Biol. 2 (1995) 758–767.
[40] W.E. Meador, A.R. Means, F.A. Quiocho, Modulation of calmodulin plasticity in molecular recognition on the basis of X-ray structures, Science 262 (1993) 1718–1721.
[41] M. Afshar, L.S. Caves, L. Guimard, R.E. Hubbard, B. Calas, G. Grassy, J. Haiech, Investigating the high affinity and low sequence specificity of calmodulin binding to its targets, J. Mol. Biol. 16 (244 (5)) (1994) 554–571.
[42] A.P. Yamniuk, H.J. Vogel, Calmodulin's flexibility allows for promiscuity in its interactions with target proteins and peptides, Mol. Biotechnol. 27 (2004) 33–57.